Phenomenological modeling of orthophosphates transfer through a nanofiltration membrane

Abdenabi Abidi[a,d,]*, Mostepha Iezid[b], Messaoud Ramdani[c], Fadhel Ismail[d], Abdelouahad Chala[e], Noureddine Gherraf[f]

[a]*Département de Génie des procédés, Université Badji Mokhtar, Annaba 23000, Algeria; Tel. +213 555 800 184;*
Tel./Fax: +213 3242 9039; email: abidi1ml@yahoo.com
[b]*Laboratoire de Génie Mécanique, Université de Biskra, Biskra, Algeria*
[c]*Laboratoire Automatique et signaux, LASA, U B M A, Annaba 23000, Algeria, email: messaoud.ramdani@univ-annaba.dz*
[d]*Laboratory LOMOP, University Badji Mokhtar of Annaba, Annaba, Algeria, email: ismail.fadhel@univ-annaba.dz*
[e]*Laboratoire de Physique des Couches Minces et Applications, Université de Biskra, Biskra, Algeria, email: chala@univ-biskra.dz*
[f]*Laboratoire des Ressources Naturelles et Aménagement des Milieux Sensibles, Larbi ben M'hidi University, Oum Elbouaghi, 04000, Algeria, email: gherraf65@gmail.com*

ABSTRACT

The present work involves the study of the potential of selective retention of orthophosphate anions $H_2PO_4^-$, HPO_4^{2-} and PO_4^{3-} in a synthetic solution and aims to a better understanding of the transport mechanisms of phosphates through a charged Nanomax-type membrane. The study deals with the Spiegler–Kedem model and its derivatives based on the thermodynamics of irreversible processes on the results of nanofiltration of model solutions depending on the charge, concentration and ionic strength. The modeling results were confirmed by the experimental values. The transport parameters namely reflection coefficient σ and solute permeability P_s could be then determined. In fact, this model established the transport parameters and predicted the intrinsic characteristics of the Nanomax-50 membrane. It was further observed that these parameters are true indicators of membrane–solute interaction reflecting the state of transport of species in a phenomenological way. The Spiegler–Kedem model seems well suited with nanofiltration of orthophosphate solutions on a Nanomax-50 type membrane.

Keywords: Nanofiltration; Orthophosphates; Nanomax-50 membrane; Transfer mechanisms; Spiegler–Kedem model

1. Introduction

Nanofiltration is a membrane separation process at the molecular level. It has the ability to selectively separate electrically charged species of small size and/or neutral molecular species. Moreover, it is very effective in removing a wide range of dissolved matter in water both organic and inorganic such as pesticides, herbicides, halogenated compounds, etc. It can operate at lower pressure compared with the reverse osmosis and thus reducing energy expenditures. The organic nanofiltration membranes are characterized by a nanometer scale pore size and have generally charged groups on surface.

The high selectivity of nanofiltration membranes is based on both size exclusion and electrostatic exclusion of charged species opposite to the membrane (Donnan mechanism).

At present, the nanofiltration membranes retention properties were studied only from macroscopic view point. In fact, several macroscopic approaches have been developed to describe the transport of material in nanofiltration membranes. The approach implicated in this study is of phenomenological order and is a direct consequence of the thermodynamics laws of irreversible processes. The resulting

* Corresponding author.

model considers the membrane as a black box between two compartments in such a way that no information regarding the membrane structure is required.

To a system consisting of a solvent and a neutral solute, Kedem and Katchalsky [1] established a phenomenological relationship of volumetric flux and solute molar flux in terms of three transport coefficients: the membrane reflection coefficient, the solute permeability and the hydraulic permeability of the membrane. The authors then extended their approach to the case of a solution containing a binary electrolyte [2]. The establishment of flow equations was based on the linear theory of thermodynamics of irreversible processes and they are applicable only for small values in both volumetric flux and the difference in transmembrane concentrations (usually not verified by nanofiltration). Spiegler and Kedem developed a procedure consisting of cutting fictitiously the membrane into a succession of elementary parts. Each part separating two fictional solution elements (with virtual concentrations slightly different from one another) is in thermodynamic equilibrium with the faces of the considered part [3]. The equations established in the framework of the linear theory of thermodynamics of irreversible processes remain, therefore, valid, but they took a local character likewise the transport coefficients. By integrating these equations over the local membrane thickness, Spiegler and Kedem set up an equation relating the solute rejection rate with the volumetric flux, the reflection coefficient, the membrane and the membrane permeability toward the solute. This model has been successfully applied in many cases and is still widely used today. The main drawback resides in the integration process of the local flow equations, which presumes that local transport coefficients are independent to virtual concentrations.

If this simplifying assumption is acceptable in the case of neutral membranes, it is most objectionable in the case of charged membranes separating solutes partially or totally ionized, except in limited cases of very low and very high volumetric fluxes [4]. The concept of membrane charge previously absent in the Spiegler–Kedem (SK) model was introduced in the expressions of the reflection coefficient and solute permeability using the theory of the fixed charge [5,6]. Nakao and Kimura [7] introduced hydrodynamic coefficients in the expressions of the reflection coefficient and solute permeability (model steric-hindrance pore [SHP]) in order to determine the structural parameters (pore radius and thickness-porosity ratio) of ultrafiltration membranes from rejection rate of neutral solutes.

Most previous work dealing with the development of the models of transport of species across membranes were based on either approaches of non-equilibrium between two phases or approaches related to the diffusion of solutes through the membrane pores [2]. Many models, supported by different considerations and assumptions have been recommended and are being developed at present [8–17].

Another approach, more mechanistic, based on the use of the extended equation of Nernst–Planck (including solute transport by convection) was proposed by Schlögl [18] by making a simplification of the thermodynamics equations of irreversible processes. The extended equation of Nernst–Planck is used in the space charge model previously developed by Morrison and Osterle [19], Gross and Osterle [20] and Fair and Osterle [21]. This model is also based on the

Navier–Stokes equations to describe the volumetric flux and on the Poisson–Boltzmann equation to find out the radial profile of the electrostatic potential within the pores.

Despite its stringency at the fundamental level, the space charge model was essentially used to study electrokinetic phenomena within cylindrical pores and has rarely been applied in the study of retention electrolytes because of the complexity of the required calculations [22,23]. Applied to the charged and selective pores, the space charge model is in fact a two-dimensional model taking into account the axial and radial variations of pressure, electrostatic potential and ion concentration inside cylindrical pores.

Various simplifications of the space charge model have been proposed to reduce the complexity and calculation time. Jacazio [24] suggested to replace the law of the Navier–Stokes by the Poiseuille equation for the description of volumetric flux while other authors made use of approximate solutions of the Poisson–Boltzmann equation [25,26].

Another approach reported by Schlögl [27] and Dresner [28] gave the possibility to simplify considerably calculations and to easily extend them to the transport of electrolytes mixtures. In this approach, the Nernst–Planck extended equation is combined with the fixed charge theory and the exclusion of solutes is governed by thermodynamic equilibria at interfaces (Donnan equilibria) and the transport inside the membrane is described by the extended Nernst–Planck equations coupled with a local condition of electroneutrality. The notion of port radius is absent and the description of transport is one-dimensional. Wang et al. [8] used this approach by introducing hydrodynamic coefficients of SHP model in the extended equation of Nernst–Planck [28,29].

In this study, the parameters of the solute–membrane system are estimated by the SK model and the SHP model (steric-pore hindrance). These two models, based on the thermodynamics of irreversible processes are combined with the film theory to facilitate estimation of the parameters, which will then be used for simulation purposes.

1.1. Theory

Nanofiltration uses membranes with the mean pore diameters less than 2 nm. Therefore, these membranes have intermediate characteristics between reverse osmosis and ultrafiltration conferring specific transport properties. The complexity of the transport mechanisms in nanofiltration may impede an optimal development of these separation techniques on an industrial scale. It is, therefore, necessary to develop simple and reliable tools to understand and predict retention properties vis-à-vis different solutes membranes.

The irreversible thermodynamics theory was first applied in the description of the transfer of solutes through a membrane by Kedem and Katchalsky [1] in the case of biological membranes, then it was expanded to the reverse osmosis membranes in 1966 [3]. This is a model "black box" without description that strictly dealt with the transport through the membrane.

When transferring each species from feed solution to permeate, the system under the influence of generalized forces passes through an endless succession of states close to equilibrium. Each new state is infinitely different from the preceding one. This model was based on the phenomenological method and relies on a linear dependence between the flux

(solvent, solute) and all the forces acting on the system: pressure gradient, electrostatic potential and chemical potential. This relationship was established through the phenomenological coefficients L_{ij} by the following equation (Eq. (1)):

$$J_i = L_{ii}F_i + \sum_{ij} L_{ij}F_j \tag{1}$$

where J_i is the flux of species i, F_i is the associated forces and F_j is the non-associated forces.

The general theory of irreversible thermodynamics was based on the assumption that each flux has a linear dependence on each force operating on the system [31]. From this premise, it is then possible to express the permeate flux J_v (Eq. (2)) and solute flux J_s (Eq. (3)) as follows [32–35]:

$$J_v = L_p(\Delta P - \sigma \Delta \pi) \tag{2}$$

$$J_s = P_s \Delta C + (1 - \sigma) C \cdot J_v \tag{3}$$

where C represents the average concentration of solute in the pores.

These expressions show two phenomenological coefficients P_s and σ. The dimensionless σ coefficient is called the reflection coefficient and is directly linked to the selectivity of membrane vis-à-vis a solute [36]. The values $\sigma = 0$ and $\sigma = 1$ correspond, respectively, to an ideally non-selective membrane (fully permeable) and an ideally selective membrane (permeable to the solvent only). P_s coefficient is in turn, considered as the permeability of solute through the membrane. Spiegler and Kedem considered that these equations became less representative to high volumetric fluxes and/or to higher concentrations gradients for which the flux of solutes may be affected. They recommended to change them by introducing local transport coefficients (Eqs. (4) and (5)):

$$J_v = -L_p \cdot \left(\frac{dp}{dx} - \sigma \frac{d\pi}{dx} \right) \tag{4}$$

$$J_s = -\bar{P} \cdot \frac{dC_s}{dx} + (1 - \sigma) \cdot C_s \cdot J_v \tag{5}$$

where L_p, p, x, π, $\bar{P}$, C_s and σ represent, respectively, the hydraulic permeability, pressure, distance, osmotic pressure, the local permeability of the solute, the solute concentration in the membrane and the reflection coefficient. The three transport parameters σ, L_p and $\bar{P}$ are needed to define the system (membrane, solute).

Assuming σ and $\bar{P}$ independent of the concentration, and putting $P = \bar{P}/Dx$, the integration of equations (Eqs. (4) and (5)) at boundary conditions ($x = 0$, $C_s = C_0$) and ($x = \Delta x$, $C_s = C_p$), combined with the equation $TR = 1 - C_p/C_o$ expressing the rejection rate [37,38] leads to the expression (Eq. (9)) relating the retention rate to the solvent flux through the membrane. Δx and P represent, respectively, the thickness of the membrane and the overall permeability.

By integration on the thickness of the membrane, L_p, $\bar{P}$ and σ are considered to be constant, we obtain Eq. (6):

$$\frac{J_V(1-\sigma)\Delta X}{\bar{P}} = \ln \frac{C_p \cdot \sigma}{C_p - C_m(1-\sigma)} \tag{6}$$

By introducing the intrinsic retention coefficient (Eq. (7)):

$$TR = \frac{(1 - \exp(J_V A))\sigma}{1 - \sigma \exp(-J_V A)} \tag{7}$$

$$A = \frac{1-\sigma}{\bar{P}}\Delta X = \frac{1-\sigma}{P_S} \tag{8}$$

Or $P_{SK} = \bar{P}/\Delta X$ is the permeability of the solute (Eq. (8)).

$$TR = 1 - \frac{1-\sigma}{1 - \sigma \exp \frac{(\sigma-1)J_v}{P_S}} \tag{9}$$

The evolution of the retention rate (TR) based on the permeate flux was chaired by the two phenomenological coefficients σ and P_s (Eq. (9)). It is, therefore, possible to determine these two coefficients from the experimental results of retention [39,40].

Note that σ is the limit value of the retention rate at high fluxes. It can be determined graphically by extrapolation with infinite flux (Eq. (10)):

$$\lim_{J_v \to \infty} TR = \sigma \tag{10}$$

P_s may, therefore, be estimated by knowing the slope of the curve $R = f(J_v)$ at low fluxes (Eq. (11)):

$$\lim_{J_v \to 0} \frac{dTR}{dJ_V} = \frac{\sigma}{P_S} \tag{11}$$

This graphical determination of σ and P_s, however, requires working in important flux ranges in order to minimize the built-in errors in various extrapolations. Their direct determination by identification between the model and experimental results (e.g., least squares method) was preferred [40].

This model permits to relate a couple (σ, P_s) to the retention of a solute, either neutral or charged, at different operating conditions (solute, membranes, solution properties, etc.). However, these phenomenological parameters cannot be used directly to understand the phenomena involved in the separation process. It is difficult to simply connect σ and P_s to the characteristics of the membrane (pore radius, charge, material, etc.) and the studied solute (hydrodynamic radius, charge, valence, etc.)

2. Experimental setup

Experiments were performed on a Millipore Proscale pilot operating in the batch circulation mode, which means that both permeate and concentrate were carried back to the vessel to maintain constant concentration in the solution to be treated. A schematic diagram of the experimental system was given in Fig. 1. The nanofiltration module was equipped with a Nanomax-50 membrane which is a composite polyamide negatively charged membrane in spiral form with a 0.37 m² area. It has a macroporous polyester mechanical support (120 μm), a microporous polysulfone intermediate structure (40 μm) and an active layer in
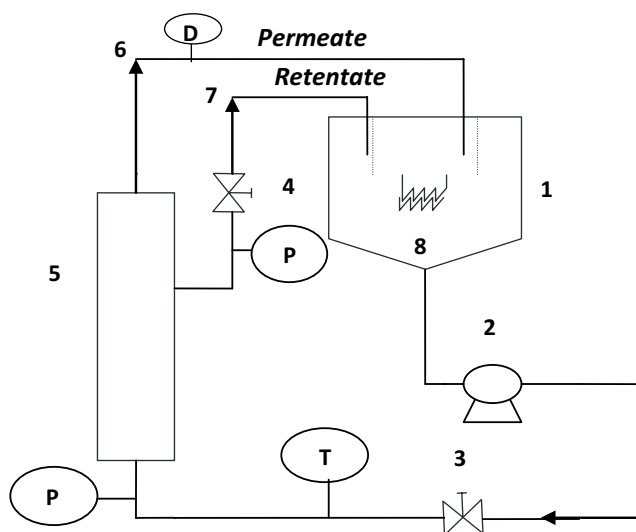
Fig. 1. Synoptic diagram of the nanofiltration pilot: 1 – feed tray; 2 – positive-displacement pump; 3 and 4 – pressure regulation valves; 5 – nanofiltration module; 6 – recirculation of permeate; 7 – recirculation of retentate; 8 – heat exchanger; D – flowmeter; P – pressure sensor; T – temperature sensor.

polybenzamide (0.4 μm). The data provided by the manufacturer reveal a cutoff about 300 Da for uncharged solutes and a pore diameter of 0.5 nm. The recommended application pressure ranges between 0 and 20 bar, the pH between 2 and 11 and the temperature must not exceed 40°C. The solutions to be treated were prepared from deionised water by adding NaH_2PO_4, Na_2HPO_4 and $NaCl$ of analytical grade (Acros Organics, Fluka Analytical). The experiments were performed at the 295 K over pressure range of 2–10 bar. The volumetric flux J_v was determined by measuring the volume of permeate collected in a given time interval, observed rejection was calculated by the relation: $TR = 1 - Cp/Co$ where C_p and C_0 are, respectively, the salt concentrations in the permeate and in the feed solution. The anions concentrations were measured by ionic chromatography using Waters 431 conductivity detector, IC-Pak Anion HR-26765 column, Waters 501 pump, eluent containing 1 L:0.32 g sodium gluconate, 0.36 g boric acid, 0.50 g sodium tetraborate decahydrate, 5 mL glycerin, 20 mL *n*-butanol, 120 mL acetonitrile and Milli-Q water.

2.1. Pressure effect

The influence of the recirculation fluxes, which is equivalent to that of the tangential flow velocity on the permeate flux was studied using the solutions of NaH_2PO_4 and Na_2HPO_4 at 100 mg (PO_4^{3-}) L^{-1}. The results obtained are shown in Figs. 2 and 3, respectively. The permeate flux increases linearly with pressure and is not affected by the recirculation flux. It remains practically independent of the tangential velocity but depends exclusively on the transmembrane pressure. Similar results were reported in the literature [41–43].

In the present study, the permeate volumetric flux increases linearly with the pressure and remains very close to the pure water flux (Figs. 2 and 3).
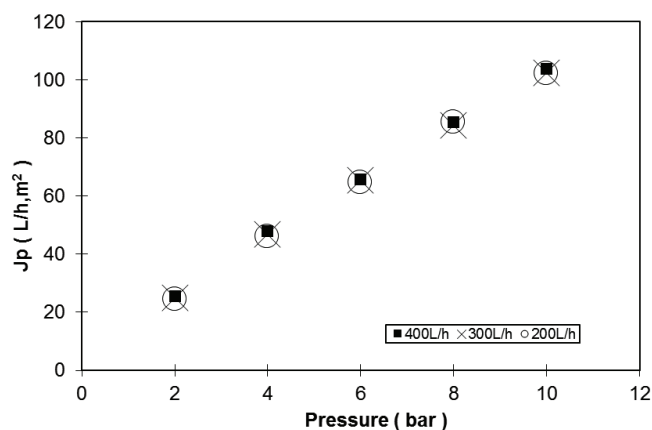

Fig. 2. Effect of pressure on the permeate fluxes of NaH_2PO_4 (100 mg (PO_4^{3-}) L^{-1}).
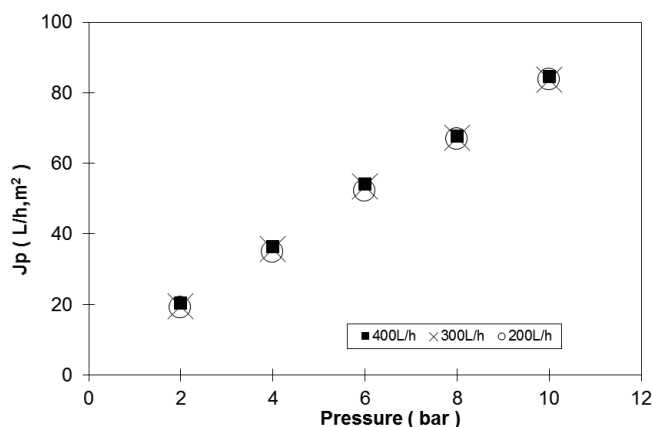

Fig. 3. Effect of pressure on the permeate fluxes of Na_2HPO_4 (100 mg (PO_4^{3-}) L^{-1}).

Authors such as Pontalier et al. [44] and Xu and Lebrun [45] considered this linearity as a result of the absence of concentration polarization where the difference between the osmotic pressure of the boundary solution and that of the bulk solution can be neglected [46]. Noting that in the rest of our study and in order to overcome its effect, the tangential flow velocity was maintained constant at a feed rate of 280 L h^{-1}.

2.2. Parameter estimation and simulation of permeate flux and rejection rates

The experimental data were obtained in several operating conditions (transmembrane pressure, initial concentration and pH) where J_v and R_{obs} were measured as a function of time. The transport parameters σ and P_s were obtained by asymptotic resolution of Eq. (9) using experimental values of J_v and TR. The obtained values of σ and P_s were considered as realistic values so as to fit experimental data with model predictions. These values were then used to simulate the flux and rejection rate under fixed conditions. The concentration polarization phenomenon was neglected considering external solutions as perfectly homogeneous. In practice,

this assumption is logical when working with large tangential flow velocities and applying moderate differences in transmembrane pressure [47].

2.3. Simulation of retention of NaH_2PO_4 and Na_2HPO_4 salts by the Spiegler–Kedem model

2.3.1. Charge effect

The pH and the nature of the ions in solution have predominant effects on the observed selectivity of the studied Nanomax-50 membrane. The orthophosphates have the particularity of having erratic charges depending on pH and the forms are interrelated through the acidity constants of phosphoric acid: $pKa_1 = 2.1$, $pKa_2 = 7.2$, $pKa_3 = 12.4$ (Fig. 4). The pH effect on the nanofiltration of orthophosphates in simple mixture has been studied by Abidi et al. [48]. This parameter can affect the properties of the membrane and the solute chemical specificities by the distribution of molecules at the interface of membrane pores and the solution, coupled with the Donnan theory. The study of the influence of pH was carried out for a phosphoric acid solution with a concentration of 100 mg L^{-1} in the presence of NaCl solution having a chloride concentration of 200 mg (Cl$^-$) L^{-1}, under a pressure of 10 bar. The temperature was fixed at 25°C. The recirculation flow was set at 280 L h^{-1} and the acidity was adjusted by the addition of NaOH. The ionization degree depends upon the nanofiltered solution pH which refers to the isoelectric point ($pI = 4.9$). This corresponds to the value of pH at which the electric charge of fixed cations neutralizes globally that of anions. The evolution of the retention of orthophosphates and chlorides ions in mixed model solutions is shown in Fig. 5. The results are discussed on the basis of three ionization cases membrane groups distinguished according to the pH of the solution.

pH > 5 (pH more than p*I*)
Since the Nanomax-50 membrane being negatively charged, owing to the ionization of RCOO$^-$ groups, the co-ions (the anions of the solution) govern the retention of the ions, as they cannot easily pass through the membrane due to repulsive interactions with membrane groups. The divalent co-ions, such as HPO$_4^{2-}$, are better retained than monovalent co-ions H$_2$PO$_4^-$ and Cl$^-$, because their strong negative charge keeps them away from the pores. In contrast, the monovalent co-ions of

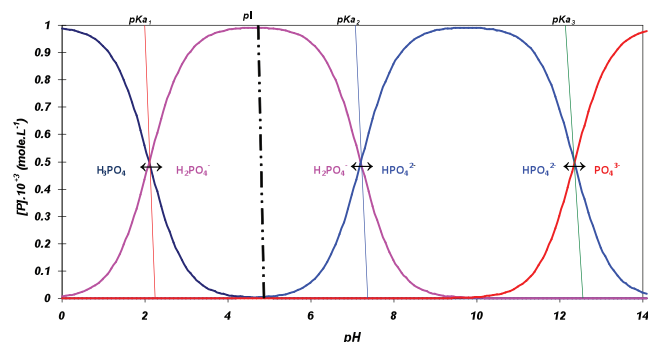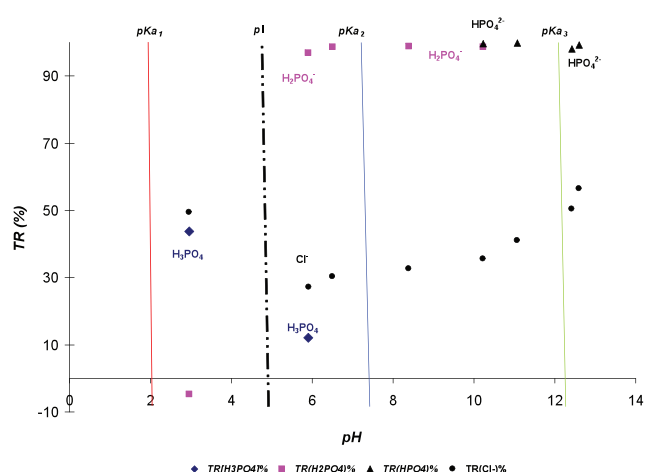Fig. 5. Retention rates of the various orthophosphates and chlorides species in a mixed solution according to pH.

higher ion mobility have lower retentions. Hence, for the same associated cation Na$^+$, Cl$^-$ retention is lower than that of H$_2$PO$_4^-$. The increase of pH with respect to phosphoric acid p*Ka* generates different forms of orthophosphates and the retention occurs in step with this variant. In fact, with pH between 6 and 7.2 (p*Ka*$_2$), the orthophosphates exist as H$_2$PO$_4^-$ and H$_3$PO$_4$ with a rejection rate of about 82% and 11%, respectively. The rejection rate of the orthophosphates increases and reaches 97% in the form of H$_2$PO$_4^-$. The H$_2$PO$_4^-$ ions are increasingly rejected by the membrane, resulting in an increase of their retention rates. This observation is apparent for pH > p*Ka*$_2$ with an equal co-existence of the two forms of phosphates H$_2$PO$_4^-$ (R = 98%) and HPO$_4^{2-}$ (R = 98%) in the retentate at pH = 10.23. Beyond this pH value, the divalent form of orthophosphates anions HPO$_4^{2-}$ dominates with a retention of about 98%. The increase in pH above the isoelectric point leads to a rise in negative charge of the membrane; hence, it is the chloride ions that are increasingly rejected by the membrane, resulting in an increase in their retention rate up to a maximum value of about 56.5%

4 < pH < 5 (pH close to p*I*)
The retention of orthophosphates by the Nanomax-50 membrane in the mixed solution is close to those determined in the simple solution. This suggests that at the isoelectric point of the membrane, the anionic groups are only weakly ionized. The observed exclusion phenomena are limited to a steric exclusion. However, at its isoelectric point, the membrane has no charge, resulted from a balance between A–NH$_3^+$ and R–COO$^-$ ionized groups.

Indeed the results presented in these figures show a minimum retention of chloride ions close to the isoelectric point, the obtained results show that the values of the orthophosphates rejection rate increased from 40% to 80% when the solution pH varies from 2.9 to 5.9. This change reflects a fluctuation of sign (positive/negative) of the membrane at the isoelectric point (p*I* = 4.9). It would then be the sieve effect which primarily governs the selectivity of the membrane due to the steric hindrance induced by the size of solute.

Fig. 4. Diagram of prevalence of the various shapes of the orthophosphoric acid according to the pH in aqueous solution.

pH < 4 (pH less than p*I*)

The membrane is positively charged and this results in a rise in the overall retention of chloride ions Cl⁻ (R = 49.36), ion exclusion effects between Na^+ and $A–NH_3^+$ groups in addition to steric exclusion effects. The reading in the diagram values shows that for pH < 4 the orthophosphates are selected as H_3PO_4 R (H_3PO_4) = 40% and a negative retention of monovalent phosphate anions R ($H_2PO_4^-$) = –5% to offset the imbalance charge created between the membrane and the solution when the pH decreases. The positive charge of the membrane increases and Na^+ ions are increasingly rejected by the $A–NH_3^+$ groups of the membrane. Although the monovalent co-ions are repelled by divalent cations to the membrane, they cross the membrane at a higher level than their concentration in the retentate, so as to compensate the charge imbalance. This transmission occurs simultaneously with that of counterions, in order to satisfy the electroneutrality condition.

Since the membrane is negatively charged, it was expected that the divalent anion HPO_4^{2-}, dominating phosphate species on the predominance diagram at pKa_2 = 7.20 < pH < pKa_3 = 12.35, will be rejected more than monovalent anion $H_2PO_4^-$, dominating at pKa_1 = 2.15 < pH < pKa_2 = 7.20. Indeed, Figs. 6–8 show that the retention of HPO_4^{2-} phosphate anions is higher than $H_2PO_4^-$ with a rate of 98% and 93%, respectively. In addition to the Donnan effect, the retention of HPO_4^{2-} may be related to the higher value of the hydrated radius (HR of HPO_4^{2-}) = 0.327 nm, (HR of $H_2PO_4^-$) = 0.302 nm [49] and to the fact that the membrane charge will be more negative at pH 8.5.

Similarly to Na_2SO_4 the retention of Na_2HPO_4 was relatively constant with changes in the permeate flux while the retention of NaH_2PO_4 increases slightly with the flux reflecting the type of force influencing the transport of each species. Comparison of the results of the SK model and experimental data shows a good fit and perfect compatibility for both phosphate salts. Transport parameters namely the reflection coefficient σ and solute permeability P_s were determined and are presented in Tables 1–3.
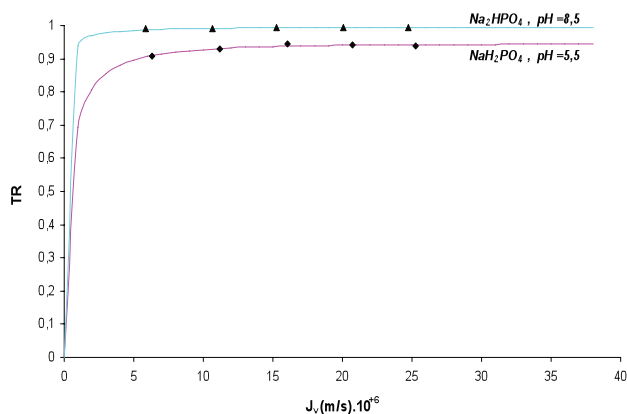
Fig. 6. Retention rate of NaH_2PO_4 and Na_2HPO_4 salts as a function of solvent flux (C_0 = 20 ppm). The lines represent the adjustment of Spiegler–Kedem model to experimental values.

Fig. 7. Retention rate of NaH_2PO_4 and Na_2HPO_4 salts as a function of solvent flux (C_0 = 100 ppm). The lines represent the adjustment of Spiegler–Kedem model to experimental values.
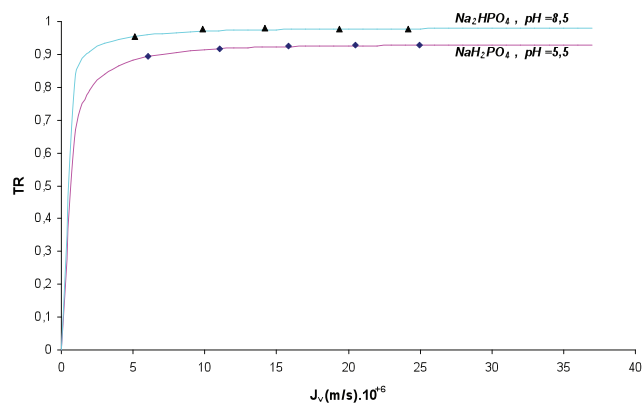
Fig. 8. Retention rate of NaH_2PO_4 and Na_2HPO_4 salts as a function of solvent flux (C_0 = 1,000 ppm). The lines represent the adjustment of Spiegler–Kedem model to experimental values.
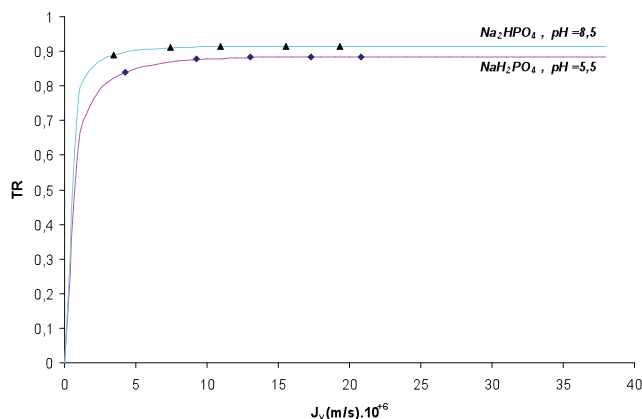
2.4. Simulation of the retention of salt NaH_2PO_4 (Spiegler–Kedem model)

2.4.1. Concentration effect

Figs. 9 and 10 show the retentions HPO_4^{2-} and $H_2PO_4^-$ anions, respectively, within a concentration range from 20 to 1,000 ppm. It was found that the retention of $H_2PO_4^-$ decreases with increasing initial concentration, while the rejection rate of HPO_4^{2-} remains almost constant despite of the variation of its initial concentration. The decrease in retention of the monovalent anion may be also attributed to the protection by the screening effect of the membrane charge by the ions in the presence of high concentration electrolytes. The increasing concentration leads to increasing formation, by counterions, of a screen neutralizing the negative charges of the membrane. Repulsion forces between the negative sites of the membrane and co-ions were then reduced. At low concentrations, the screen effect was very low and the repulsion of anions is important and leads to high retention. When the concentration was higher, the screen effect was amplified and the potential of the membrane decreases. Accordingly, the repulsion

Table 1
Evaluation of the coefficient of reflection σ and specific permeability P_s by the model of Spiegler–Kedem for salts: NaH_2PO_4 and Na_2HPO_4 (C_0 = 20 ppm)

Solute	σ	P_s (m/s) × 10^7
NaH_2PO_4	0.9438	3.90039
Na_2HPO_4	0.9951	0.45007

Table 2
Evaluation of the coefficient of reflection σ and specific permeability P_s by the model Spiegler–Kedem for salts: NaH_2PO_4 and Na_2HPO_4 (C_0 = 100 ppm)

Solute	σ	P_s (m/s) × 10^7
NaH_2PO_4	0.9284	4.18277
Na_2HPO_4	0.9796	1.76865

Table 3
Evaluation of the coefficient of reflection σ and specific permeability P_s by the model of Spiegler–Kedem for salts: NaH_2PO_4 and Na_2HPO_4 (C_0 = 1,000 ppm)

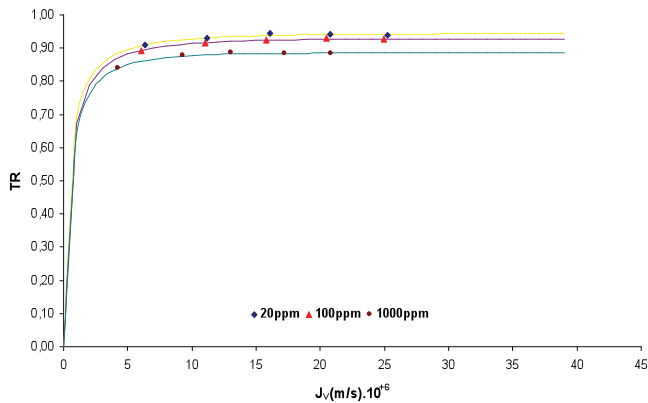| Solute	σ	P_s (m/s) × 10^7
NaH_2PO_4	0.8850	4.30854
Na_2HPO_4	0.9145	2.11395

Fig. 9. Effect of concentration on retention rate of NaH_2PO_4 salt. The lines represent the adjustment of Spiegler–Kedem model to experimental values.

between the membrane and co-ions decreases. In fact, these co-ions crossed the membrane more easily, bringing with them the counterions in order to meet electroneutrality, and hence the retention was reduced. The regression parameters σ and P_s for both phosphate salts are shown in Table 4.

2.5. Simulation of the retention of NaH_2PO_4 salt by Spiegler–Kedem model

2.5.1. Effect of ionic strength

The effect of the ionic strength was studied by adding various concentrations of NaCl ranging from 20 to 500 ppm.
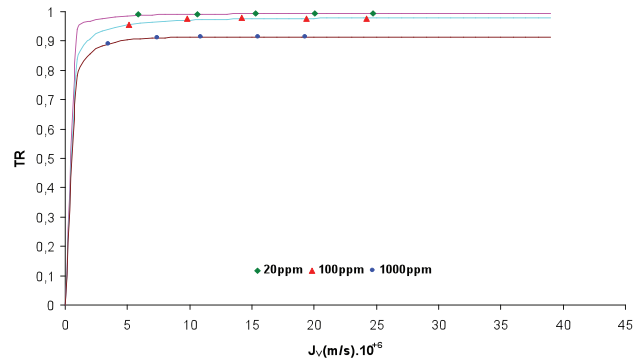

Fig. 10. Effect of concentration on the retention rate of Na_2HPO_4 salt. The lines represent the adjustment of Spiegler–Kedem model to experimental values.

Table 4
Evaluation of reflection coefficient σ and specific permeability P_s by Spiegler–Kedem model for NaH_2PO_4 and Na_2HPO_4 salts

Solute	Concentration (ppm)	σ	P_s (m/s) × 10^7
NaH_2PO_4	20	0.9438	3.90039
	100	0.9284	4.18277
	1,000	0.8850	4.30854
Na_2HPO_4	20	0.9951	0.45007
	100	0.9796	1.76865
	1,000	0.9145	2.11395

Fig. 11. Effect of ionic strength on retention rate of NaH_2PO_4 salt. The lines represent the adjustment of Spiegler–Kedem model to experimental values.

Figs. 11 and 12 show that the retention of phosphate anions decreases with increasing NaCl concentration. This well known behavior is a characteristic of charged membranes and is generally interpreted by the screening phenomenon. Increasing the concentration of the sodium ions against Na^+ in the solution leads to the progressive formation of a negative charge neutralizer screen membrane. As the total
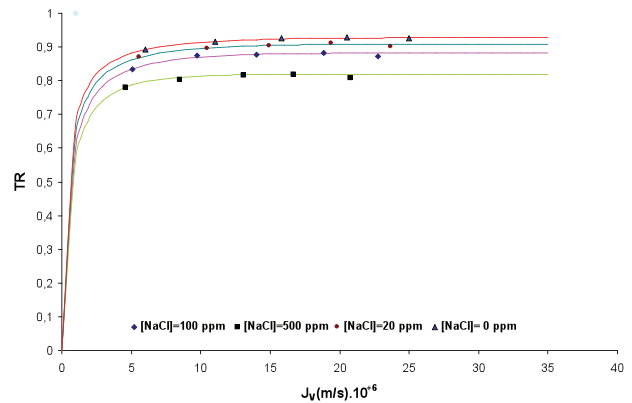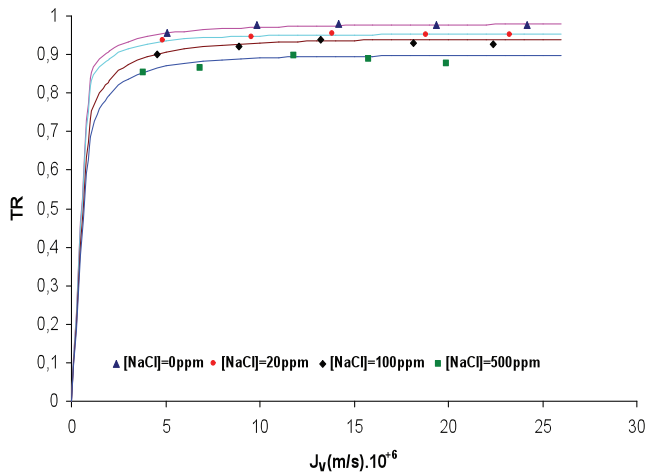
Fig. 12. Effect of ionic strength on retention rate of Na_2HPO_4 salt. The lines represent the adjustment of Spiegler–Kedem model to experimental values.

Table5
Evaluation of the coefficient of reflection σ and specific permeability P_s by Spiegler–Kedem model for NaH_2PO_4 and Na_2HPO_4 salts in the presence of NaCl

Solute	Concentration (ppm)	σ	P_s (m/s) × 10^7
NaH_2PO_4NaCl	0	0.9284	4.18277
	20	0.9093	4.68627
	100	0.8825	5.3303
	500	0.8192	5.37675
Na_2HPO_4NaCl	0	0.9796	1.76865
	20	0.9524	1.87501
	100	0.9398	3.10563
	500	0.8967	3.53215

charge of the membrane decreases, the electrostatic effect of the membrane becomes lower and accordingly, a decrease in the retention of phosphate anions occurs. The figures represent the approximation of the retention of phosphate anions by the SK model with the most appropriate values of σ and P_s. Nevertheless, the results show a good fit of the model for all concentrations of NaCl discussed with phosphate anions $H_2PO_4^-$ and HPO_4^{2-}. The estimated transport parameters are given in Table 5. Reading of σ and P_s values shows their dependence on the concentration of NaCl. Indeed, σ decreases and P_s increases with increasing concentration of NaCl.

3. Results

The study of the transport of orthophosphates ions through a nanofiltration membrane of Nanomax-50 type is divided into several parts:

- The first was devoted to the study of solute transport through a charged organic nanofiltration membrane (with an active polybenzamide layer). The SK model was

used to investigate the transport properties of NaH_2PO_4 and Na_2HPO_4. Retention properties vis-à-vis binary electrolyte membranes are then studied. The study highlighted the amphoteric surface sites of the active layer and indicated that the Donnan exclusion played a major role in the membrane exclusion mechanism. The phenomenological SK model was used to describe the experimental results. The adjustment of the theoretical curves on the rates of experimental rejections allowed access to transport parameters (σ and P_s) for the studied salts. The results showed that the permeability P_s varies inversely with the reflection coefficient σ meaning that the more the ion has a low permeability, the better it will be rejected. This explained the displacement of the membrane retention in the ascending order of the feed and the valence of the anions and cations. In fact, σ depends on the nature of the co-ion. It is particularly important when the co-ion is strongly negatively charged.

- The study of the transport of electrolytes (NaH_2PO_4 and Na_2HPO_4) at different concentrations was performed by estimating σ and P_s from the adjustment of the SK model to the experimental values. The predictions of an SK-type model are confronted to the rate of experimental ionic rejection rates. It should be noted that a satisfactory description of the experimental results was obtained for the two electrolytes at different concentrations. The results in the table show that when the concentration of phosphate salts increases, the specific permeability of the ion also increases, resulting in a decrease of the reflection coefficient, and therefore, a considerable decrease in the selectivity of the membrane. This result confirmed our assumptions given in the experimental section and confirmed what are found in the literature [50,51]. In fact, Perry and Linder [52] showed that the increase in salt concentration results in a decrease of the reflection coefficient and an increase in permeability, and explained their results by the Donnan exclusion which interprets these findings by screen effect.

- The transport parameters σ and P_s vary with pH. The increase in pH of the phosphate salt led to an increase in reflection coefficient σ and a decrease in permeability P_s. It was also noted that σ was greater for pH higher than pI and the results are in agreement with the experimental results.

- The change in the ionic composition by adding sodium chloride to phosphate salts generated the concept of ionic strength that occurred in complex solutions. The adjustment of the SK model on the experiment produces transport parameters σ and P_s which are characteristics of these conditions.

- The results underlined the importance of Donnan exclusion phenomenon in the case of nanofiltration of phosphates in complex mixtures. In fact, the reflection coefficient σ decreases and the specific permeability P_s increases with increase in the NaCl concentration.

- The reflection coefficient σ depends on the nature of the co-ion. In fact, the results showed that σ (HPO_4^{2-}) > σ ($H_2PO_4^-$). In the case of monovalent co-ions, the variation of reflection coefficient highlights the effect of parameters other than the co-ions charge density, on the selectivity of the membrane.

4. Conclusion

The objective of this work was to suggest models for understanding the mechanisms of transfer. We have presented some models based on irreversible thermodynamics theory. It was observed that the model used suits well the separations based on Nanomax-50 membrane. Indeed this model has allowed us to determine the transport parameters (σ and P_s) of phosphate salt solutions and also the prediction of the intrinsic characteristics of the Nanomax-50 membrane. It should be noted that these parameters are true indicators of membrane–solute interaction reflecting the state of transport of species in a phenomenological way. The model SK seems well suited to nanofiltration of phosphate solutions on an organic membrane Nanomax-50 type. Moreover, it was easy to deduce the analytical forms of the permeate flux which allows access to the volume fraction profile. Once the model becomes predictive, it is possible to consider its use in the continuous monitoring of nanofiltration of such molecules by measurements and calculation of standard sizes. We can as well consider optimal conduction of the filtering operation in terms of permeate flux vs. the energy required to bring the solution to flow and create the appropriate transmembrane pressure gradient.

References

[1] O. Kedem, A. Katchalsky, Thermodynamic analysis of the permeability of biological membranes to non-electrolytes, Biochim. Biophys. Acta, 27 (1958) 229–246.
[2] O. Kedem, A. Katchalsky, Permeability of composite membranes. Part I? Electric current, volume flow and flow of solute through membranes, Trans. Faraday Soc., 59 (1963) 1918–1930.
[3] K.S. Spiegler, O. Kedem, Thermodynamics of hyperfiltration (reverse osmosis): criteria for efficient membranes, Desalination, 1 (1966) 311–326.
[4] X. Lefebvre, Study of Transfer Models in Nanofiltration, Application of the Hybrid Model Based on Equations of Nernst-Planck Extended by the Development of the Simulation "Nanoflow", PhD Thesis, University of Montpellier II, France, 2003 (in French).
[5] E. Hoffer, O. Kedem, Hyperfiltration in charged membranes: the fixed charge model, Desalination, 2 (1967) 25–39.
[6] S. Kimura, I. Jitsuhara, Transport through charged ultrafiltration membranes, Desalination, 46 (1983) 407–416.
[7] S. Nakao, S. Kimura, Models of membrane transport phenomena and their applications for ultrafiltration data, J. Chem. Eng. Jpn., 15 (1982) 200–205.
[8] X.L. Wang, T. Tsuru, M. Togoh, S.I. Nakao, S. Kimura, Transport of organic electrolytes with electrostatic and steric-hindrance effects through nanofiltration membranes, J. Chem. Eng. Jpn., 28 (1995) 372–380.
[9] X. Xu, H.G. Spencer, Transport of electrolytes through a weak acid nanofiltration membrane: effects of flux and crossflow velocity interpreted using a fine-porous membrane model, Desalination, 113 (1997) 85–93.
[10] J. Schaep, C. Vandecasteele, A.W. Mohammad, R. Bowen, Modelling the retention of ionic component for different nanofiltration membranes, Sep. Purif. Technol., 22–23 (2001) 169–179.
[11] I. Koyuncu, D. Topacik, Effect of organic ion on the separation of salts by nanofiltration membranes, J. Membr. Sci., 195 (2002) 247–263.
[12] A. Szymczyk, P. Fievet, Investigating transport properties of nanofiltration membranes by means of a steric, electric and dielectric exclusion model, J. Membr. Sci., 252 (2005) 77–88.
[13] J.A. Otero, G. Lena, J.M. Colina, P. Prádanos, F. Tejerina, A. Hernández, Characterisation of nanofiltration membranes structural analysis by the DSPM and microscopical techniques, J. Membr. Sci., 279 (2006) 410–417.
[14] J.L.C. Santos, P. de Beukelaar, I.F.J. Vankelecom, S. Velizarov, J.G. Crespo, Effect of solute geometry and orientation on the rejection of uncharged compounds by nanofiltration, Sep. Purif. Technol., 50 (2006) 122–131.
[15] A.I. Cavaco Morão, A. Szymczyk, P. Fievet, A.M. Brites Alves, Modelling the separation by nanofiltration of a multi-ionic solution relevant to an industrial process, J. Membrane Sci., 322 (2008) 320–330.
[16] B. Cuartas-Uribe, M.C. Vincent-Vela, I. Álvarez-Blanco, M.I. Alcaina-Miranda, E. Soriano-Costa, Nanofiltration of sweet whey and prediction of lactose retention as a function of permeate flux using the Kedem–Spiegler and Donnan Steric Partining models, Sep. Purif. Technol., 56 (2007) 38–46.
[17] A.M. Hidalgo, G. León, M. Gómez, M.D. Murcia, E. Gómez, J.L. Gómez, Application of the Spiegler–Kedem–Kachalsky model to the removal of 4-chlorophenol by different nanofiltration membranes, Desalination, 315 (2013) 70–75.
[18] R. Schlögl, Transport of Substances Through Membranes, Dr. Dietrich Steinkopff Publishing House, Darmstadt, 1964.
[19] F.A. Morrison, J.F. Osterle, Electrokinetic energy conversion in ultrafine capillaries, J. Chem. Phys., 43 (1965) 2111.
[20] R.J. Gross, J.F. Osterle, Membrane transport characteristics of ultrafine capillaries, J. Chem. Phys., 49 (1968) 228.
[21] J.C. Fair, J.F. Osterle, Reverse electrodialysis in charged capillary membranes, J. Chem. Phys., 54 (1971) 3307–3316.
[22] P. Neogi, E. Ruckenstein, Viscoelectric effects in reverse osmosis, J. Colloid Interface Sci., 79 (1981) 159–169.
[23] X.L. Wang, T. Tsuru, S.I. Nakao, S. Kimura, Electrolyte transport through nanofiltration membranes by the space-charge model and the comparison with Teorell-Meyer-Sievers model, J. Membr. Sci., 103 (1995) 117–133.
[24] G. Jacazio, R.F. Probstein, A.A. Sonin, D. Yung, Electrokinetic salt rejection in hyperfiltration through porous materials. Theory and experiment, J. Phys. Chem., 76 (1972) 4015–4023.
[25] H.J.M. Hijnen, J. Van Daalen, J.A.M. Smit, The application of the space-charge model to the permeability properties of charged microporous membranes, J. Colloid Interface Sci., 107 (1985) 525–539.
[26] A.E. Yaroshchuk, S.S. Dukhin, Phenomenological theory of reverse osmosis in macroscopically homogeneous membranes and its specification for the capillary space-charge model, J. Membr. Sci., 79 (1993) 133–158.
[27] R. Schlögl, Membrane permeation in systems far from equilibrium, Ber. Bunsen.-Ges. Phys. Chem., 70 (1966) 400–414.
[28] L. Dresner, Some remarks on the integration of the extended Nernst-Planck equations in the hyperfiltration of multicomponent solutions, Desalination, 10 (1972) 27–46.
[29] L. Dresner, Stability of the extended Nernst-Planck equations in the description of hyperfiltration through ion-exchange membranes, J. Phys. Chem., 76 (1972) 2256–2267.
[30] W.R. Bowen, H.R. Mukhtar, Characterisation and prediction of separation performance of nanofiltration membranes, J. Membr. Sci., 112 (1996) 263–274.
[31] C. Vidal, G. Dewel, P. Borckmans, Au-delà de l'équilibre, Beyond Balance, Hermann, 1994.
[32] M. Pontié, H. Buisson, C.K. Diawara, H. Essis-Tome, Studies of halide ions mass transfer in nanofiltration — application to selective defluorination of brackish drinking water, Desalination, 157 (2003) 127–134.
[33] N.N. Li, A.G. Fane, W.S.W. Ho, T. Matsuura, Advanced Membrane Technology and Application, John Wiley & Sons, Inc., Publications, New York, 2008.
[34] B. Van der Bruggen, M. Manttari, M. Nyström, Drawbacks of applying nanofiltration and how to avoid them: a review, Sep. Purif. Technol., 63 (2008) 251–263.
[35] F. Peng, X. Huang, A. Jawor, E.M.V. Hoek, Transport, structural, and interfacial properties of poly(vinyl alcohol)–polysulfone composite nanofiltration membranes, J. Membr. Sci., 353 (2010) 169–176.
[36] A. Bhattacharya, P. Ghosh, Nanofiltration and reverse osmosis membranes: theory and application in separation of electrolytes, Rev. Chem. Eng., 20 (2004) 111–173.

[37] V.L. Golovashin, S.I. Lazarev, M. Mamantov, Kinetic characteristics of reverse-osmosis separation of an aqueous solution of aniline in a flat-frame apparatus, Russ. J. Appl. Chem., 78 (2005) 1096–1100.

[38] K. Kosutic, B. Kunst, Removal of organics from aqueous solutions by commercial RO and NF membranes of characterized porosities, Desalination, 142 (2002) 47–56.

[39] K. Mehiguene, S. Taha, N. Gondrexon, J. Cabon, G. Dorange, Copper transfer modeling through a nanofiltration membrane in the case of ternary aqueous solution, Desalination, 127 (2000) 135–143.

[40] S. Nakao, S. Kimura, Analysis of solute rejection in ultrafiltration, J. Chem. Eng. Jpn., 14 (1981) 32–37.

[41] M.D. Afonso, M.N. de Pinho, Transport of $MgSO_4$, $MgCl_2$, and Na_2SO_4 across an amphoteric nanofiltration membrane, J. Membr. Sci., 179 (2000) 137–154.

[42] A.C. Gomez, I.C. Goncalvez, M.N. de Pinho, The role of adsorption on nanofiltration of azo dyes, J. Membr. Sci., 255 (2005) 157–167.

[43] N. Ben Fares, S. Taha, G. Dorange, Influence of the operating conditions on the elimination of zinc ions by nanofiltration, Desalination, 185 (2005) 245–253.

[44] P.Y. Pontalier, A. Ismail, M. Ghoul, Study of the influence of conditions on the selective separation of ions by nanofiltration membranes, Cahier scientifique, 112 (1995) 642–644.

[45] Y. Xu, R.E. Lebrun, Comparison of nanofiltration properties of two membranes using electrolyte and non-electrolyte solutes, Desalination, 122 (1999) 95–105.

[46] I.M. Noel, R. Lebrun, C.R. Bouchard, Electro-nanofiltration of a textile direct dye solution, Desalination, 129 (2000) 125–136.

[47] S. Déon, P. Dutournié, P. Fievet, L. Limousy, P. Bourseau, Concentration polarization phenomenon during the nanofiltration of multi-ionic solutions: influence of the filtrated solution and operating conditions, Water Res., 47 (2013) 2260–2272.

[48] A. Abidi, N. Gherraf, S. Ladjel, M. Rabiller-Baudry, T. Bouchami, Effect of operating parameters on the selectivity of nanofiltration phosphates transfer through a Nanomax-50 membrane, Arabian J. Chem., 9 (2016) S334–S341.

[49] M.Y. Kiriukhin, K.D. Collins, Dynamic hydration numbers for biologically important ions, Biophys. Chem., 99 (2002) 155–168.

[50] J. Gilron, N. Gara, O. Kedem, Experimental analysis of negative salt rejection in nanofiltration membranes, J. Membr. Sci., 185 (2001) 223–236.

[51] G.T. Ballet, A. Hafiane, M. Dhahbi, Influence of operating conditions on the retention of phosphate in water by nanofiltration, J. Membr. Sci., 290 (2007) 164–172.

[52] M. Perry, C. Linder, Intermediate reverse osmosis ultrafiltration (RO UF) membranes for concentration and desalting of low molecular weight organic solutes, Desalination, 71 (1989) 233–245.